Title
Poly(lactide-co-glycolide) microspheres for MRI-monitored transcatheter delivery of sorafenib to liver tumors.

Journal
Journal of controlled release : official journal of the Controlled Release Society, 184(1)

ISSN
0168-3659

Authors
Chen, Jeane
Sheu, Alexander Y
Li, Weiguo
et al.

Publication Date
2014-06-01

DOI
10.1016/j.jconrel.2014.04.008

Peer reviewed

Published in final edited form as:
J Control Release. 2014 June 28; 184: 10–17. doi:10.1016/j.jconrel.2014.04.008.

Poly(lactide-*co*-glycolide) Microspheres for MRI-Monitored Transcatheter Delivery of Sorafenib to Liver Tumors

Jeane Chen, B.S.[1,2], **Alexander Y. Sheu, B.S**[2], **Weiguo Li, Ph.D**[2], **Zhuoli Zhang, MD, Ph.D**[2,3], **Dong-Hyun Kim, Ph.D**[2], **Robert J. Lewandowski, MD**[2,3], **Reed A. Omary, MD, MS**[2,3,4], **Lonnie D. Shea, Ph.D**[1,3], and **Andrew C. Larson, Ph.D**[2,3,4,5]

[1]Department of Chemical & Biological Engineering, Northwestern University, Evanston, IL, USA

[2]Department of Radiology, Northwestern University, Chicago, IL, USA

[3]Robert H. Lurie Comprehensive Cancer Center of Northwestern University, Chicago, IL, USA

[4]Department of Biomedical Engineering, Northwestern University, Chicago, IL, USA

[5]Department of Electrical Engineering and Computer Science, Evanston, IL, USA

Abstract

The multi-kinase inhibitor (MKI) sorafenib can be an effective palliative therapy for patients with hepatocellular carcinoma (HCC). However, patient tolerance is often poor due to common systemic side effects following oral administration. Local transcatheter delivery of sorafenib to liver tumors has the potential to reduce systemic toxicities while increasing the dose delivered to targeted tumors. We developed sorafenib-eluting PLG microspheres for delivery by intra-hepatic transcatheter infusion in an orthotropic rodent HCC model. The particles also encapsulated iron-oxide nanoparticles permitting magnetic resonance imaging (MRI) of intra-hepatic biodistributions. The PLG microspheres (diameter ≈1 μm) were loaded with 18.6% (w/w) sorafenib and 0.54% (w/w) ferrofluid and 65.2% of the sorafenib was released within 72 hours of media exposure. *In vitro* studies demonstrated significant reductions in HCC cell proliferation with increasing doses of the sorafenib-eluting microspheres, where the estimated IC_{50} was a 29 ug/mL dose of microspheres. During *in vivo* studies, MRI permitted intra-procedural visualization of intra-hepatic microsphere delivery. At 72 hours after microsphere infusion, microvessel density was significantly reduced in tumors treated with the sorafenib-eluting microspheres compared to both sham control tumors (by 35%) and controls (by 30%). These PLG microspheres offer the potential to increase the efficacy of molecularly targeted MKI therapies while reducing systemic exposures via selective catheter-directed delivery to HCC.

All correspondence should be directed to: Andrew Larson, Ph. D., 737 North Michigan Avenue, Suite 1600, Chicago, IL 60611, Phone: (312) 926-3499, Fax: (312) 926-5991, a-larson@northwestern.edu.

Keywords

sorafenib; hepatocellular carcinoma; magnetic resonance imaging; poly(lactide-*co*-glycolide)

INTRODUCTION

The FDA recently approved the multi-kinase inhibitor (MKI) sorafenib tosylate (common name sorafenib, trade name Nexavar®, Bayer) for treating patients with unresectable hepatocellular carcinoma (HCC) ([1]). Sorafenib has a proven survival benefit ([2]) in patients with advanced stage disease and is now the standard of care for those patients ([3–5]). Sorafenib inhibits angiogenesis via blockage of VEGF and PDGF receptors and cell proliferation via blockage of B-Raf and C-Raf of the Map Kinase pathway ([2, 6–8]). Currently, sorafenib is administered orally and thus, can lead to side effects including hand and foot syndrome, diarrhea, and hypertension ([2, 4, 9]). The severity of these side effects (estimated to occur in roughly 30% of patients ([2, 9]) often results in sorafenib dose reductions or discontinuation.

Transcatheter arterial chemoembolization (TACE)([10]) is commonly is used for palliative treatment of HCC to prevent systemic exposure of chemotherapeutics for HCC. TACE involves selective placement of an arterial catheter to deliver drugs and embolic materials directly into the vascular blood supply of hepatic tumor(s). More recently developed transcatheter techniques for the treatment of HCC include radioembolization with Y-90 microspheres ([5, 10–13]) and another form of chemoembolization wherein drug eluting beads (sulfonate modified polyvinyl alcohol hydrogel microspheres) are selectively infused for both embolization and locally sustained delivery of doxorubicin to the targeted vascular beds ([12, 14–17]).. Similar microsphere drug delivery platforms could potentially increase the efficacy of sorafenib therapy for HCC while reducing systemic exposures via catheter-directed delivery.

The purpose of our study was to investigate the feasibility of sorafenib-eluting poly(D,L-lactide-co-glycolide) (PLG) microspheres for transcatheter delivery. PLG is a biocompatible polymer widely used to encapsulate therapeutic drugs for sustained delivery ([18–20]) and is advantageous in that it can be formulated as an injectible particle that encapsulates both hydrophobic and hydrophilic components for localized drug delivery for localized drug delivery ([18, 19, 21]). Furthermore, the PLG microspheres co-encapsulate a ferrofluid of iron-oxide nanoparticles, thus permitting MRI of intra-hepatic biodistributions. While a number of imaging approaches have been employed with PLG microspheres, MRI does not require exposure to ionizing radiation and provides excellent soft tissue contrast for depicting tumor tissues. We evaluated sorafenib elution properties and *in vitro* cell cytotoxicity after exposure to these microspheres. We then investigated the *in vivo* therapeutic efficacy of these sorafenib-eluting PLG microspheres following transcatheter infusion in rodent HCC models. The MR relaxivity properties of these microspheres were characterized with phantom studies prior to *in vivo* MRI studies validating the potential to visualize selective delivery to HCC in rodent models.

MATERIALS AND METHODS

Materials

75:25 Poly (D,L-lactide-*co*-glycolide) (PLG RESOMER® RG 752H, MW=4000–15000) was purchased from Sigma Aldrich (St. Louis, MO). Sorafenib tosylate was purchased from LC Laboratories (Woburn, MA). Ferrofluid (EMG 304) was provided by Ferrotec (Santa Clara, CA).

Microsphere Fabrication

Microspheres were fabricated via a double emulsion/solvent evaporation method modified from that described by DeFail et al ([22]). PLG polymer (250 mg) was dissolved in 0.8 mL of a 1:6 solution of dimethyl sulfoxide: dichloromethane and then combined with a 10 mg/mL solution of sorafenib dissolved in 4 mL of DMSO and 100 μL of ferrofluid. The solution was emulsified by vortexing for 5 sec before adding 2 mL of 1% polyvinyl alcohol. This solution was vortexed again for 15 sec and poured into a beaker containing 50 mL of 0.3% polyvinyl alcohol. The microspheres were stirred in the beaker for 3hrs before centrifugation for 10 min. Finally, the microspheres were washed 3 times with deionized water before freezing and lyophilization.

Characterization of Microsphere Size and Morphology

Microsphere morphology was characterized using a Leica DM IL inverted contrasting microscope equipped with a Leica DFC290 Camera (Leica Microsystems, Wetzlar, Germany) as well as a FEI Tecnai Spirit G2 Transmission Electron Microscope (TEM) (Hillsboro, OR). After lyophilization, microspheres were suspended in water for analysis with a nano-s zetasizer (Malvern Instruments Ltd., UK) to determine size characteristics.

Characterization of Microsphere Sorafenib Content

Microsphere sorafenib content was characterized using high performance liquid chromatography (HPLC) with methods adapted from Blanchet et al. ([23]). The microspheres were dissolved in solution of 1% DMSO in 60:40 acetonitrile:ammonium acetate at a 1 mg/mL concentration and centrifuged to pellet the polymer and ferrofluid. The supernatant was analyzed for sorafenib concentrations using an Agilent 1260 Infinity Quaternary LC HPLC (Santa Clara, CA) system and Zorbax C18 column. The weight percentage of sorafenib in the microspheres (total percentage of microsphere mass contributed by encapsulated sorafenib) was calculated as the ratio between the sorafenib concentration measured with HPLC and the 1 mg/mL concentration of PLG microspheres in the original sample. The loading efficiency was calculated as the ratio between the weight percentage of sorafenib in the microspheres and the overall weight percentage of sorafenib included originally during fabrication (roughly 9.66%).

Characterization of Microsphere Ferrofluid Content

The ferrofluid content of the microspheres was characterized using inductively coupled plasma mass spectometry (ICP-MS). ICP-MS measurements were performed using a ThermoFisher X Series II system (Thermo Fisher Scientific, USA). In triplicate,

microspheres were digested in nitric acid at a concentration of 2 mg/mL and prepared in a 2% nitric acid buffer solution with 5 ppb Yttrium as an internal standard. The ferrofluid weight percentage (total percentage of microsphere mass contributed by the encapsulated ferrofluid) was determined as ratio of the concentration of ferrofluid determined from our ICP-MS measurements to the original 2 mg/mL microsphere sample. Loading efficiency was calculated as the ratio between the weight percentage of ferrofluid in the microspheres and the overall weight percentage of ferrofluid included originally during fabrication (roughly 29.95%).

Characterization of T2 Relaxivity Properties

Quantitative R_2 relaxivity measurements were performed using 1% agar phantoms that included increasing concentrations of the PLG microspheres (0–2 mg/mL). A 7.0-Tesla MRI scanner (Bruker Clinscan, Billerica, MA) was used for both phantom and subsequent *in vivo* imaging studies. These phantom studies were performed using a Carr-Purcell-Meiboom-Gill (CPMG) sequence (TR=1000ms, 1.5 mm slice thickness, 6 TE ranging from 10 to 60 ms). R_2 time constants were determined by fitting signal decay curves to mono-exponential function: $S(TE) = M_o e^{-TE/T2}$. We calculated the Pearson correlation coefficient between microsphere concentration and resultant R2 values and associated linear least squares fit line with slope of this line providing the relaxivity value: $\Re$ = R_2 relaxivity in units of $msec^{-1}$ $(mg\ sphere)^{-1}mL$.

In Vitro Characterization of Sorafenib Release Rates

We used 5 mg samples of the microspheres placed in 50 mL tubes with 50 mL of 1% SDS in PBS release media. These conical tubes were placed on an orbital shaker rotating at 120 rpm within incubator maintained at 37°C. Over the course of one week, 1 mL aliquots were repeatedly collected from each tube for analysis with a LAMBDA 1050 UV/Vis/NIR spectrophotometer (Perkin Elmer) at a wavelength of 255 nm.

In Vitro Response Studies

In order to verify retention of sorafenib potency post-microsphere fabrication, and to validate efficacy of sorafenib against an established rat hepatoma cell line, McA-RH7777 rat hepatoma cells were exposed to one of four different doses of sorafenib-eluting PLG microspheres (equivalent to sorafenib doses of 0, 2, 4, and 6 μg/mL) over 3 different exposure periods (24, 48, and 72 hrs), each study repeated in quadruplicate. 50,000 cells were plated in 2 mL of Dulbecco's Modified Eagles Medium (DMEM). After reaching 50% confluence (1–2 days), cells were washed and treated with a solution of sorafenib-eluting PLG microspheres in a 2 mL solution of DMEM corresponding to doses described above. For control studies (no microsphere exposure) the cells were treated with a 2 mL solution of DMEM with 0.1% (*v/v*) DMSO. After completion of the prescribed exposure period for a given sample, the cells were washed twice with PBS, trypsinized, and collected for counting with a Countess® Automated Cell Counter (Invitrogen Corp., Carlsbad, CA); these cell counts were used to compare dose dependent cell proliferation rates and estimate IC_{50}.

Creation of Animal Model

Studies were performed with approval from Institutional Animal Care and Use Committee (IACUC). McA-RH7777 rat hepatoma cells were suspended in media and directly injected into the left lateral liver lobe during mini-laparotomy procedures in 18 male Sprague Dawley rats. Tumors were allowed to grow for 7 days to reach a size typically >5 mm in diameter. These rats were separated into three groups: untreated control group (6 rats), sham control group that was administered ferrofluid-only PLG microspheres (6 rats), and treatment group that was administered microspheres containing both ferrofluid and sorafenib (6 rats). The latter two groups underwent hepatic arterial catheterization procedures for microsphere administration after 7 days.

Catheterization Procedures

Sham control and treatment rats both underwent procedures to invasively catheterize the proper hepatic artery ([24, 25]). The catheterization procedure involved surgically exposing the portal triad above the first loop of the duodenum. Afterwards, the common hepatic artery was then clamped with a vascular clamp to temporarily prevent bleeding and a 4-0 suture used to permanently ligate the gastroduodenal artery to prevent backwards flow of the microspheres to the bowels. A 24 gauge microcatheter (Terumo SurFlash®, Somerset, NJ) was inserted distal to this ligation point in the gastroduodenal artery. The catheter is then guided into the proper hepatic artery from the gastroduodenal artery after which, 0.1 mL of heparin was infused followed by a 4 mg dose of the sorafenib-eluting PLG microspheres; each infusion was followed by a 0.2 mL saline flush and there was a minimal residual dose left undelivered. The catheter was then withdrawn, and a 3-0 suture then used to permanently ligate the gastroduodenal artery above the insertion position to prevent bleeding. The animals were then moved to the MRI scanner located adjacent to the surgical suite.

In Vivo MRI of Microsphere Delivery to Liver Tumors

Baseline scans were performed immediately prior to catheterization and microsphere infusion procedures (described above) and follow-up scans performed immediately afterwards in coronal orientation using a multi-slice T_2-weighted spin-echo sequence with following parameters: TR/TE=1,300/10 ms, 0.7 mm slice thickness, FOV 71×85 mm, 216×256 matrix, respiratory triggering with MRI-compatible small animal gating system (Model 1025, SA Instruments, Stony Brook, NY).

Histology and Immunohistochemistry

Three days after catheterization and imaging procedures, each rat was euthanized. Livers were harvested and tumor-containing segments resected for microtome sectioning. 5 μm slices through the center of each tumor were used for both hematoxylin and eosin (H&E) and Prussian blue staining (providing confirmation of ferrofluid-containing microsphere delivery). Additional slices were used for rat anti-CD34 staining and microvessel density (MVD) measurements. All slides were digitized at x200 optical magnification using a TissueFAXS microscope (TissueGnostics GmbH, Vienna, Austria). Post-processing was performed using the HistoQuest software package (TissueGnostics GmbH). Post-processing

steps involved digitally stitching together the individual images acquired with the TissueFAXs microscope to produce a signal image depicting the entire specimen on each slide. From this compiled image, the tumor was selected with manual delineation of a region of interest (ROI). Tissues within this ROI were evaluated with an automated threshold analysis approach to identify areas stained brown thus indicating positive staining of CD34. We then calculated the percentage of the ROI stained positively for CD34, our quantitative estimate for MVD. The HistoQuest software was used to measure the tumor area within each immunohistochemistry slide.

Statistical Analysis

Analyses were performed using Stata (StataCorp LP, College Station, TX) software. All results are presented as mean±standard deviation (SD) as indicated. One-way ANOVA with Scheffe post-hoc correction and student's unpaired t-test were used to compare MVD measurements in control, sham, and treatment group animals. Tests were considered statistically significant with a p-value<0.05.

RESULTS

Microsphere Characterization Studies

The PLG microspheres were morphologically spherical in shape (Fig. 1A), and had a mean diameter of 0.98+/− 0.10 μm (Fig. 1B).

The weight percentage of sorafenib included in the microspheres (total percentage of microsphere mass contributed by encapsulated sorafenib) was 18.6% (w/w). The weight percentage of ferrofluid included in the microspheres (total percentage of microsphere mass contributed by encapsulated ferrofluid) was 0.54% (w/w), which corresponds to a loading efficiency of 1.8%. The drug release profile determined from these subsequent sorafenib-eluting microsphere indicated that 65.2% of the encapsulated sorafenib was released within the initial 72 hrs of media exposure (Fig. 2).

Microspheres loaded with the ferrofluid could be detected by MRI imaging, as illustrated by the T_2-weighted image depicting 1% agar phantoms with ferrofluid-loaded PLG microsphere concentrations from 0–2 mg/mL (Fig. 3A). T_2-weighted signal decay rates increased with increasing microsphere concentration (Fig. 3B). The calculated R_2 values increased linearly with microsphere concentration (Fig. 3C), $r^2 = 0.989$. The R_2 relaxivity for these microspheres was determined to be 0.0224 $msec^{-1}$ $(mg\ sphere)^{-1}$ mL. A comparison between R2 values for an agar phantom that included free ferrofluid as opposed to encapsulated ferrofluid demonstrated that the former induces more rapid T2 signal decay (R2 = 0.027 ms^{-1} versus 0.0097 ms^{-1} for 0.69 μg mass within a 1 mL volume of agar).

In Vitro Cytotoxicity Studies

In vitro cell proliferation studies demonstrated significant reductions in rat hepatoma cell proliferation with exposure to increasing doses of the sorafenib-eluting microspheres (Fig. 4). The IC_{50} for these sorafenib-eluting PLG microspheres was determined to be 29 μg/mL. According to our prior drug encapsulation studies, this dose of microspheres would provide

5.4 μg/mL of sorafenib, which is comparable to the IC_{50} determined previously during *in vitro* sorafenib response studies in Hep G2 and PLC\PRF\5 cell lines ([7, 8]).

In Vivo Catheterization and MRI of Microsphere Delivery

Subsequent studies investigated the localization of microspheres to a rat model of HCC. Rats were inoculated with tumor cells, and microspheres were injected after 1 week. Prior to microspheres infusion, tumors could be observed as they were hyperintense compared to surrounding liver tissues in T2-weighted images (Fig. 5A). Tumors were present in 18 of 20 animals with sizes ranging from 2.5 to 8.1 mm in diameter. A representative T2-weighted image acquired immediately after transcatheter PLG microsphere infusion indicates microspheres within the tumor (Fig. 5B). Intra-hepatic microsphere delivery was restricted to the targeted tumor-bearing liver lobe with positions of microsphere deposition observed as punctate local reductions to the signal intensity within the T2-weighted images.

The MRI observation that microspheres deposit within the liver was confirmed with histological staining of the tissue for iron with Prussian blue. Prussian blue staining in tissues from treated rats confirmed successful microsphere delivery to targeted tumors (Fig. 6). Representative slides depicting anti-CD34 IHC staining of endothelial cells in tumor tissue specimens from untreated control, sham control, and treatment group animals indicate differences in response with regard to angiogenesis (Fig. 7).

Overall, a qualitatively appreciable reduction in CD34 expression was observed within specimens from treated tumors compared to control. Micro-vessel density, estimated as the ratio between CD34 positive stained areas and the total tumor area, was significantly higher in control group tumors (4.10 ± 0.69, mean±SD) relative to sorafenib-eluting microspheres (2.86±1.82, mean±SD) ($p<0.01$). Similarly, sham control tumors had a greater density (4.41±1.42, mean±SD) than tumors from animals treated with the sorafenib-eluting microspheres ($p<0.01$). No significant difference was observed between the micro-vessel density in control and sham control tumor specimens ($p=0.65$). The sorafenib treated tumors had cross-sectional areas of 13.6±6.4 mm^2 (mean±SD), while the control had cross-sectional areas of 16.2±7.2 mm^2 (mean±SD), and the sham control group had cross-sectional areas of 10.2±3.5 mm^2 (mean±SD). There was no significant difference between the sorafenib treated group and each control group ($p>.05$).

Discussion

Sorafenib has demonstrated clinical efficacy for the treatment of advanced HCC. However, the commonly unacceptable side-effects following oral administration have limited patient tolerance ([2, 4, 9]). Furthermore, low serum levels in some patients suggest that the systemic bioavailability of sorafenib following oral administration may not be adequate to consistently elicit a potent therapeutic response [26]. Transcatheter delivery of sorafenib via drug-eluting microspheres should improve the efficacy of sorafenib therapy while limiting systemic toxicities. For our current studies, sorafenib-eluting PLG microspheres were synthesized using double emulsion/solvent evaporation methods. The therapeutic efficacy of these microspheres was demonstrated *in vitro* during cell culture studies and *in vivo* using orthotropic rodent HCC models. Follow-up *in vivo* MRI studies validated that the intra-

hepatic biodistribution of these microspheres could be readily visualized due to the co-encapsulation of an iron-oxide ferrofluid.

A reduction in angiogenesis (30% decrease in microvessel density compared to controls) was demonstrated 72 hrs following transcatheter delivery of these sorafenib-eluting PLG microspheres in rodent HCC models. These findings importantly demonstrate the potential to use this PLG microsphere drug delivery system to elicit the intended *in vivo* response. For these studies, a 72hr (3 day) follow-up interval was chosen based upon the sorafenib release profile of the synthesized microspheres (during *in vitro* studies, a plateau in the release profile was clearly evident after 3-days of media exposure and cumulative release of roughly 65% of the encapsulated sorafenib).

While there was no statistical significance between the tumor cross-sectional areas between the treatment groups, sorafenib is used primarily as a cytostatic therapy, therefore tumor size changes were not expected to change over the relatively short 72 hr follow-up interval. Additional investigations evaluating therapeutic responses at both earlier and later follow-up intervals as well as the therapeutic responses elicited when using a broad range of different microsphere doses and/or sorafenib release rates will be valuable.

Hydrogel embolic microspheres ([5, 12, 14–17]) have been widely employed for transcatheter delivery of doxorubicin to HCC. However, given poor water solubility, sorafenib cannot be readily loaded into these hydrogel platforms. Herein, PLG was employed for microsphere fabrication, with the hydrophobic drug sorafenib dissolved along with the polymer in the organic phase. This approach enabled loading of sorafenib into a particle platform with high efficiencies. Hydrophobic drug loading in PLG is well studied and in comparison to previous literature with sorafenib for other applications, the loading efficiency was comparable to studies performed by Butoescu et al. ([27, 28]), and greater than that observed in a sorafenib dextran/PLG nanoparticle study by Kim et al.([29]). The relatively poor solubility of sorafenib dictated a need for relatively large volumes of DMSO during our current microsphere fabrication process; this fabrication process resulted in the fabrication of roughly 1 micron microspheres. Prior studies in rodent liver tumor models suggest that smaller microspheres are more distally distributed following intra-arterial infusion with a greater volume of these smaller microspheres reaching the targeted tumor tissues (compared to larger microspheres). ([30]). However, smaller microsphere sizes can increase the potential for lung shunting. Taking each of these factors into account, we considered a microsphere size of roughly one micron acceptable for these initial feasibility studies, particularly given the limited number of prior studies rigorously comparing size-dependent microsphere distributions following intra-arterial infusion in liver tumor rat models. Future studies rigorously comparing size-dependent distal distribution of these PLG microspheres in both rodents and larger mammals are now highly warranted; clinical translation of these techniques will likely require modification of current fabrication processes for improved mono-dispersity.

Microspheres have previously been labeled with nuclear SPECT, PET, x-ray and magnetic resonance imaging (MRI) agents for pre-clinical and clinical *in vivo* imaging however, the developed microspheres for TACE procedures have yet to labeled with imaging agents. As

TACE procedures employ rigorous imaging techniques to ensure proper catheter placement, the ability to image the sorafenib-loaded microspheres through the encapsulated ferrofluid may facilitate the assessment of delivery efficiency.

Iron oxide-based agents have been widely used for MR imaging; however, a majority of these agents have only been used in pre-clinical research settings. One pertinent limitation is that these agents are typically sequestered by the reticuloendothelial system in the liver thus slowing clearance rates. Additionally, iron-oxide agents are negative contrast agents essentially reducing local signal with T_2-weighted images (as opposed to enhancing signal). Given the endogenous iron content of the liver, T_2-weighted signal intensities are already significantly reduced thus somewhat limiting the dynamic range of induced signal reductions possible upon deposition of iron-oxide contrast materials. Alternative options that could readily be considered for labeling PLG microspheres include chelated gadolinium agents for T_1-weighed MRI, barium or iodinated agents for CT, or radioactive agents for PET or SPECT modalities.

The susceptibility differences between the microspheres and adjacent tissues produces magnetic field gradients with a spatial extent much larger than the individual microspheres. These local field gradients induce a more rapid T_2 decay within voxels containing the microspheres. It is the latter effect that was visualized during these studies, rather than direct visualization of individual microspheres (given the much larger size of each voxel relative to the size of individual microspheres). Larger microspheres should contain a larger volume of ferrofluid and hence should produce stronger local field and correspondingly stronger T_2 contrast. However, similar T_2 contrast may also occur due to the presence of multiple smaller microspheres within a single voxel. Due to the inability to image individual microspheres with MRI methods, we cannot draw definitive conclusions regarding the impact of microsphere size upon resulting visibility within the acquired T_2-weighted images. For these studies, the observed contrast within these T_2-weighted images most likely resulted from the deposition of a broad range of different microsphere sizes within each voxel.

Our imaging studies demonstrated that the intra-hepatic biodistribution of these microspheres was well depicted during subsequent *in vivo* MRI studies. When imaging at higher field strengths (3–7 Tesla), small amounts of ferrofluid impart large local magnetic field gradients; the resulting local dephasing of both static and diffusing spins can then be detected as marked signal decay within T_2-weighted images. While quantitative R_2 measurements were not performed during the current *in vivo* MRI studies, the linear relationship between R_2 and microsphere concentration (demonstrated during phantom studies) suggests the potential to perform quantitative measurements of microsphere delivery to liver tumors. Ultimately, for clinical translation, additional studies will be necessary at lower magnetic field strengths (1.5T and 3.0T) more commonly used clinically. The relaxivity of superparamagnetic iron-oxide agents generally scales with field strength ([30]); thus, additional studies will be necessary to validate the potential to detect these ferrofluid-containing PLG microspheres at clinical field strengths.

Conclusions

In conclusion, these studies demonstrated that PLG microspheres can be produced with encapsulated sorafenib and ferrofluid for MRI monitored, transcatheter delivery to liver tumors. *In vitro* and *in vivo* studies demonstrated potent therapeutic responses. These polymer microsphere drug delivery platforms could increase the efficacy of molecularly targeted MKI therapies while reducing systemic exposures via selective catheter-directed delivery.

References

1. Ravikumar K, et al. Sorafenib and its tosylate salt: a multikinase inhibitor for treating cancer. Acta Crystallogr C. 2011; 67(Pt 1):8.
2. Llovet JM, et al. Sorafenib in advanced hepatocellular carcinoma. N Engl J Med. 2008; 359(4):378–90. [PubMed: 18650514]
3. Forner A, Llovet JM, Bruix J. Hepatocellular carcinoma. The Lancet. 379(9822):1245–1255.
4. Keating GM, Santoro A. Sorafenib: A Review of its Use in Advanced Hepatocellular Carcinoma. Drugs. 2009; 69(2):223–240.10.2165/00003495-200969020-00006. [PubMed: 19228077]
5. de Lope CR, et al. Management of HCC. Journal of Hepatology. 2012; 56(Supplement 1)(0):S75–S87. [PubMed: 22300468]
6. Wysocki PJ. Targeted therapy of hepatocellular cancer. Expert Opinion on Investigational Drugs. 2010; 19(2):265–274. [PubMed: 20074016]
7. Li Liu YC, Chen Charles, Zhang Xiaomei, McNabola Angela, Wilkie Dean, Wilhelm Scot, Lynch Mark, Carter Christopher. Sorafenib blocks the RAF/MEK/ERK pathway, inhibits tumor angiogenesis, and induces tumor cell apoptosis in hepatocellular carcinoma model PLC/PRF/5. Cancer Research. 2006; 66:8.
8. Wilhelm S, et al. Discovery and development of sorafenib: a multikinase inhibitor for treating cancer. Nat Rev Drug Discov. 2006; 5(10):835–44. [PubMed: 17016424]
9. Cheng AL, et al. Efficacy and safety of sorafenib in patients in the Asia-Pacific region with advanced hepatocellular carcinoma: a phase III randomised, double-blind, placebo-controlled trial. Lancet Oncol. 2009; 10(1):25–34. [PubMed: 19095497]
10. Lencioni R. Loco-regional treatment of hepatocellular carcinoma. Hepatology. 2010; 52(2):762–73. [PubMed: 20564355]
11. Lewandowski RJ, et al. Radioembolization with 90Y microspheres: angiographic and technical considerations. Cardiovasc Intervent Radiol. 2007; 30(4):571–92. [PubMed: 17516113]
12. Lewandowski RJ, et al. Transcatheter intraarterial therapies: rationale and overview. Radiology. 2011; 259(3):641–57. [PubMed: 21602502]
13. Kennedy A, et al. Radioembolization for the treatment of liver tumors general principles. Am J Clin Oncol. 2012; 35(1):91–9. [PubMed: 22363944]
14. Liapi E, et al. Drug-Eluting Particles for Interventional Pharmacology. Techniques in Vascular and Interventional Radiology. 2007; 10(4):261–269. [PubMed: 18572139]
15. Lewis A, et al. Doxorubicin eluting beads – 1: Effects of drug loading on bead characteristics and drug distribution. Journal of Materials Science: Materials in Medicine. 2007; 18(9):1691–1699. [PubMed: 17483878]
16. Lewis AL, et al. DC bead: in vitro characterization of a drug-delivery device for transarterial chemoembolization. J Vasc Interv Radiol. 2006; 17(2 Pt 1):335–42. [PubMed: 16517780]
17. Liapi E, Geschwind JF. Intra-arterial therapies for hepatocellular carcinoma: where do we stand? Ann Surg Oncol. 2010; 17(5):1234–46. [PubMed: 20405328]
18. Jain RA. The manufacturing techniques of various drug loaded biodegradable poly(lactide-co-glycolide) (PLGA) devices. Biomaterials. 2000; 21(23):2475–90. [PubMed: 11055295]

19. Wischke C, Schwendeman SP. Principles of encapsulating hydrophobic drugs in PLA/PLGA microparticles. International Journal of Pharmaceutics. 2008; 364(2):298–327. [PubMed: 18621492]
20. Whittlesey KJ, Shea LD. Delivery systems for small molecule drugs, proteins, and DNA: the neuroscience/biomaterial interface. Experimental Neurology. 2004; 190(1):1–16. [PubMed: 15473976]
21. Jain R, et al. Controlled Drug Delivery by Biodegradable Poly(Ester) Devices: Different Preparative Approaches. Drug Development and Industrial Pharmacy. 1998; 24(8):703–727. [PubMed: 9876519]
22. Defail AJ, et al. Controlled release of bioactive doxorubicin from microspheres embedded within gelatin scaffolds. J Biomed Mater Res A. 2006; 79(4):954–62. [PubMed: 16941588]
23. Blanchet B, et al. Validation of an HPLC-UV method for sorafenib determination in human plasma and application to cancer patients in routine clinical practice. Journal of Pharmaceutical and Biomedical Analysis. 2009; 49(4):1109–1114. [PubMed: 19278805]
24. Garin E, et al. Description and technical pitfalls of a hepatoma model and of intra-arterial injection of radiolabelled lipiodol in the rat. Lab Anim. 2005; 39(3):314–20. [PubMed: 16004691]
25. Sheu AY, et al. Invasive catheterization of the hepatic artery for preclinical investigation of liver-directed therapies in rodent models of liver cancer. Am J Transl Res. 2013; 5(3):269–78. [PubMed: 23634238]
26. Ghassabian S, et al. Role of human CYP3A4 in the biotransformation of sorafenib to its major oxidized metabolites. Biochem Pharmacol. 2012; 84(2):215–23. [PubMed: 22513143]
27. Butoescu N, et al. Dexamethasone-containing biodegradable superparamagnetic microparticles for intra-articular administration: physicochemical and magnetic properties, in vitro and in vivo drug release. Eur J Pharm Biopharm. 2009; 72(3):529–38. [PubMed: 19303928]
28. Butoescu N, et al. Co-encapsulation of dexamethasone 21-acetate and SPIONs into biodegradable polymeric microparticles designed for intra-articular delivery. J Microencapsul. 2008; 25(5):339–50. [PubMed: 18465308]
29. Kim do H, et al. Antitumor activity of sorafenib-incorporated nanoparticles of dextran/poly(dl-lactide-co-glycolide) block copolymer. Nanoscale Res Lett. 2012; 7(1):7–91. [PubMed: 22221425]
30. Deckers F, et al. The influence of MR field strength on the detection of focal liver lesions with superparamagnetic iron oxide. Eur Radiol. 1997; 7(6):887–92. [PubMed: 9228104]

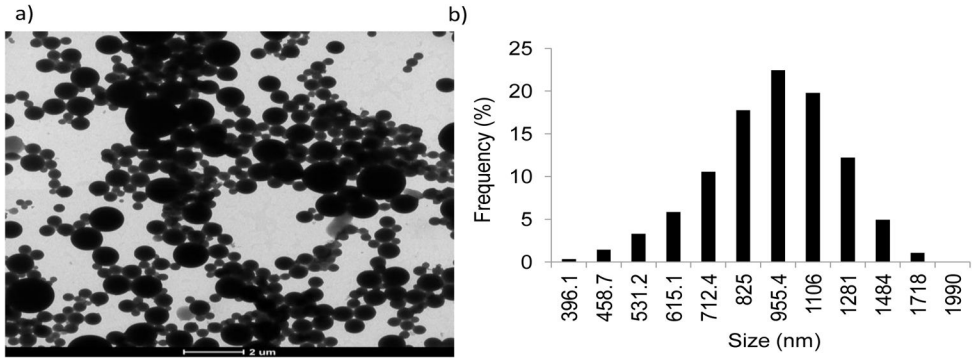

Figure 1.

TEM image of PLGA microspheres encapsulating both sorafenib and ferrofluid (**A**). Histogram depicting the size distribution of these PLG microspheres (**B**).

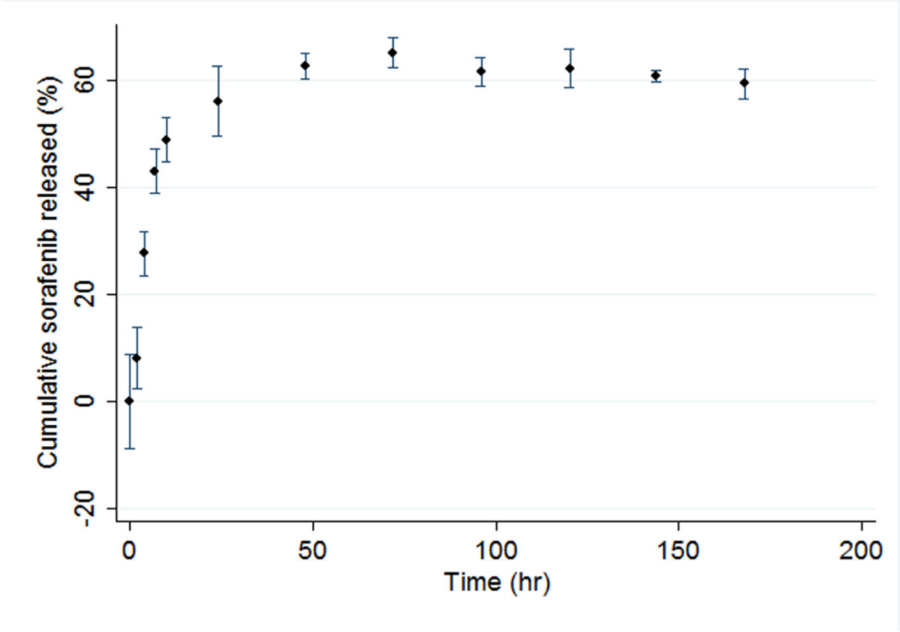

Figure 2.
Sorafenib release profile for PLG microspheres in 1% SDS in PBS at 37°C.

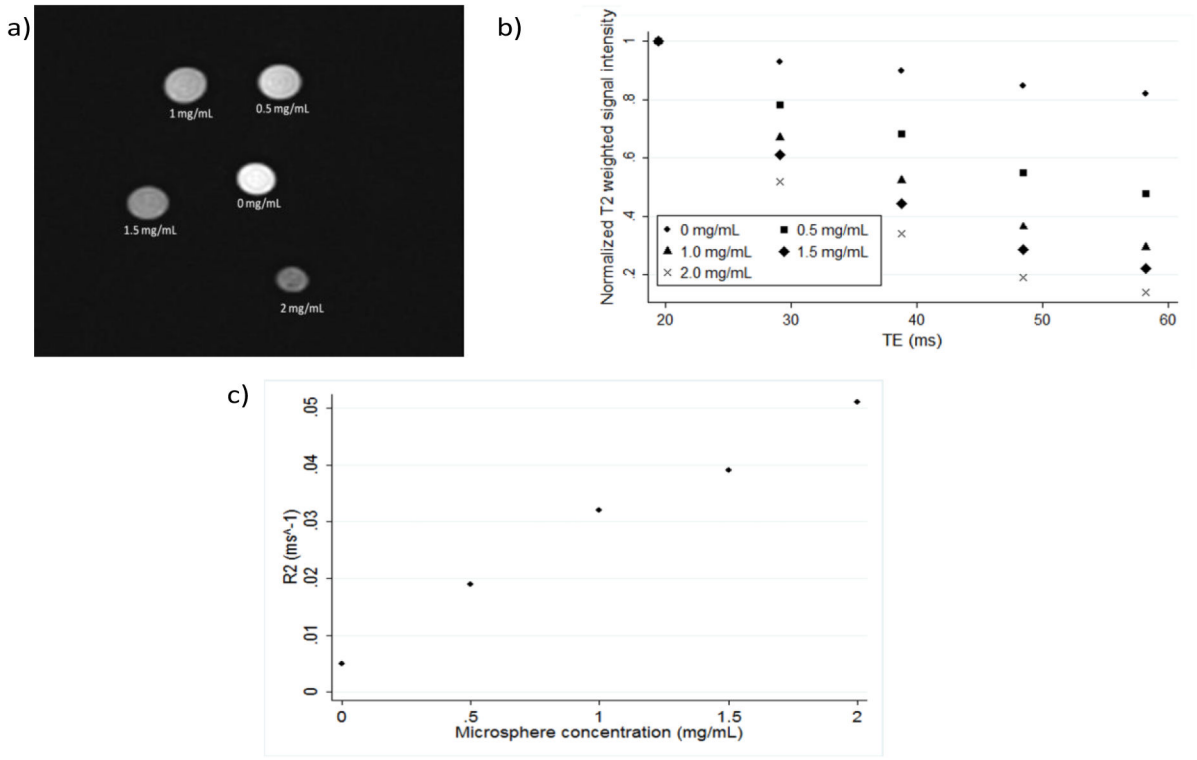

Figure 3.

T2-weighted image of agar phantoms including ferrofluid-loaded PLG microsphere concentrations ranging from 0 to 2 mg/mL (**A**). T2-weighted signal decay rates increased in proportion to ferrofluid-loaded PLG microsphere concentration (**B**). Plot depicting the resulting linear relationship between quantitative R2 measurements and corresponding microsphere concentration for each phantom (r^2>0.98) (**C**).

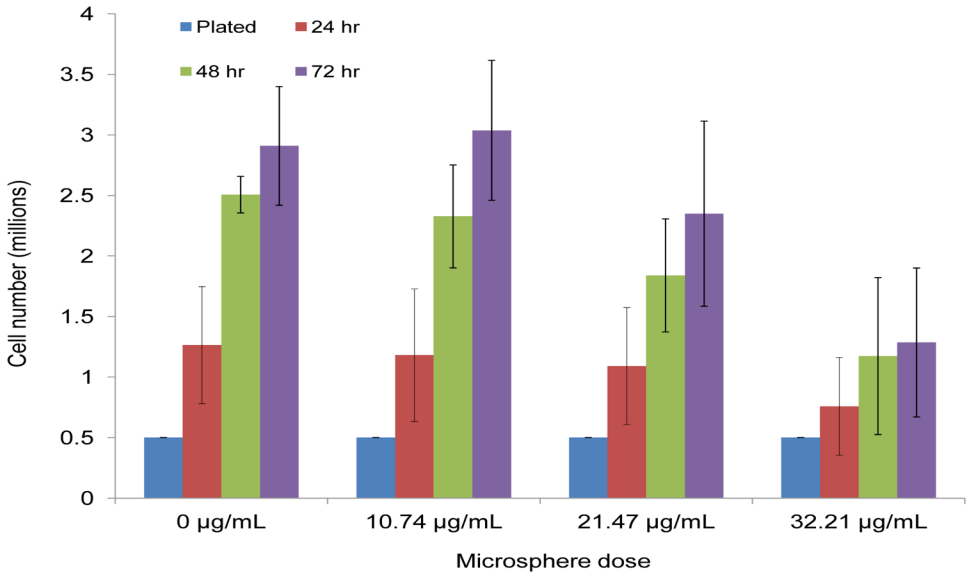

Figure 4.

McA-RH7777 rat hepatoma cell counts after 24, 48, and 72 hours *in vitro* exposure to increasing dose concentrations of the sorafenib-eluting PLG microspheres.

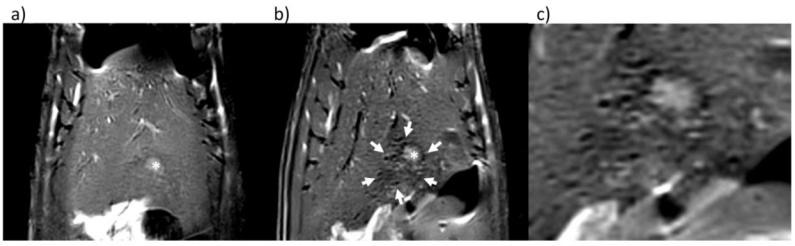

Figure 5.

Coronal T_2-weighted images acquired before (**A**) and after (**B**) transcatheter infusion of PLG microspheres co-encapsulating sorafenib and ferrofluid (asterisk denotes position of tumor within left hepatic lobe). Intra-hepatic microsphere deposition was depicted as punctate regions of signal loss within the T_2-weighted images post-infusion (arrows, **B**). A magnified image of the tumor region from the post-procedural T_2-weighted MRI scan is provided in panel **C**.

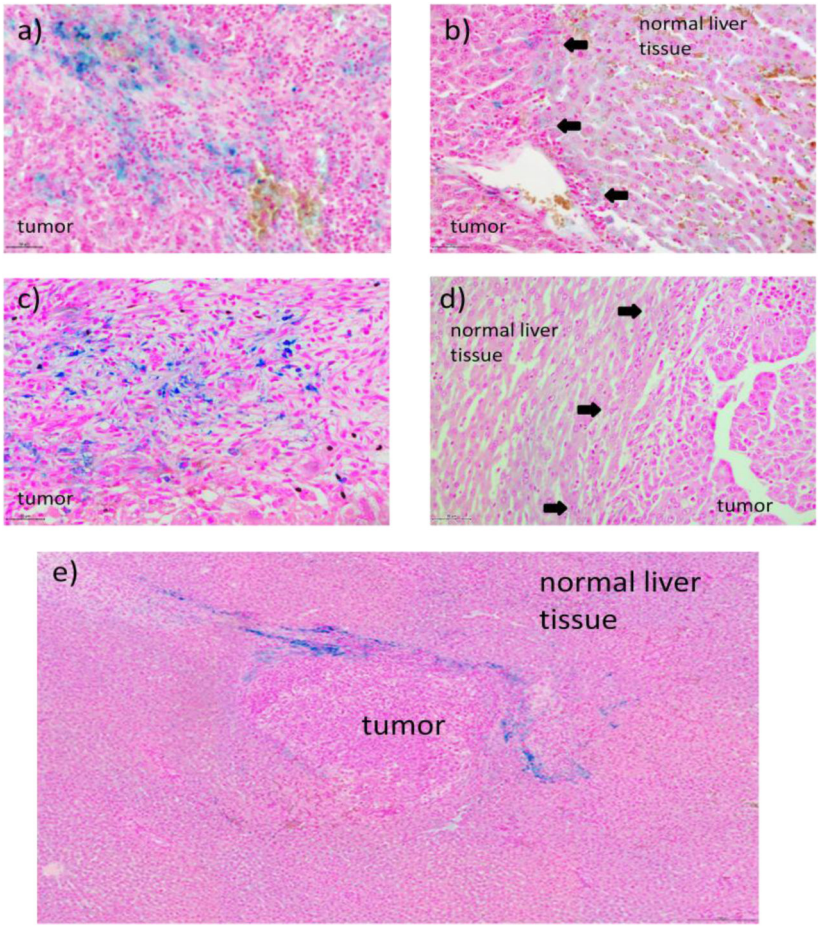

Figure 6.

Prussian blue staining of treated tumor tissues confirmed selective delivery of the ferrofluid-loaded PLG microspheres (blue ferrofluid deposits well depicted within 200x magnification image from representative histology slide) (**A**). A region depicting both tumor and adjacent normal liver tissues from a treatment group animal is shown in panel **B** (200x magnification, arrows denote the border between the normal and tumor tissues). Prussian blue histology slide from sham control animal similarly depicts intra-tumoral microsphere deposition (**C**). Prussian blue staining was not observed in histology slides from control group animals, the representative example in panel **D** (200x magnification) depicts border between tumor and adjacent normal liver tissues. A whole tumor image for a sorafenib-treated rat is shown in panel E.

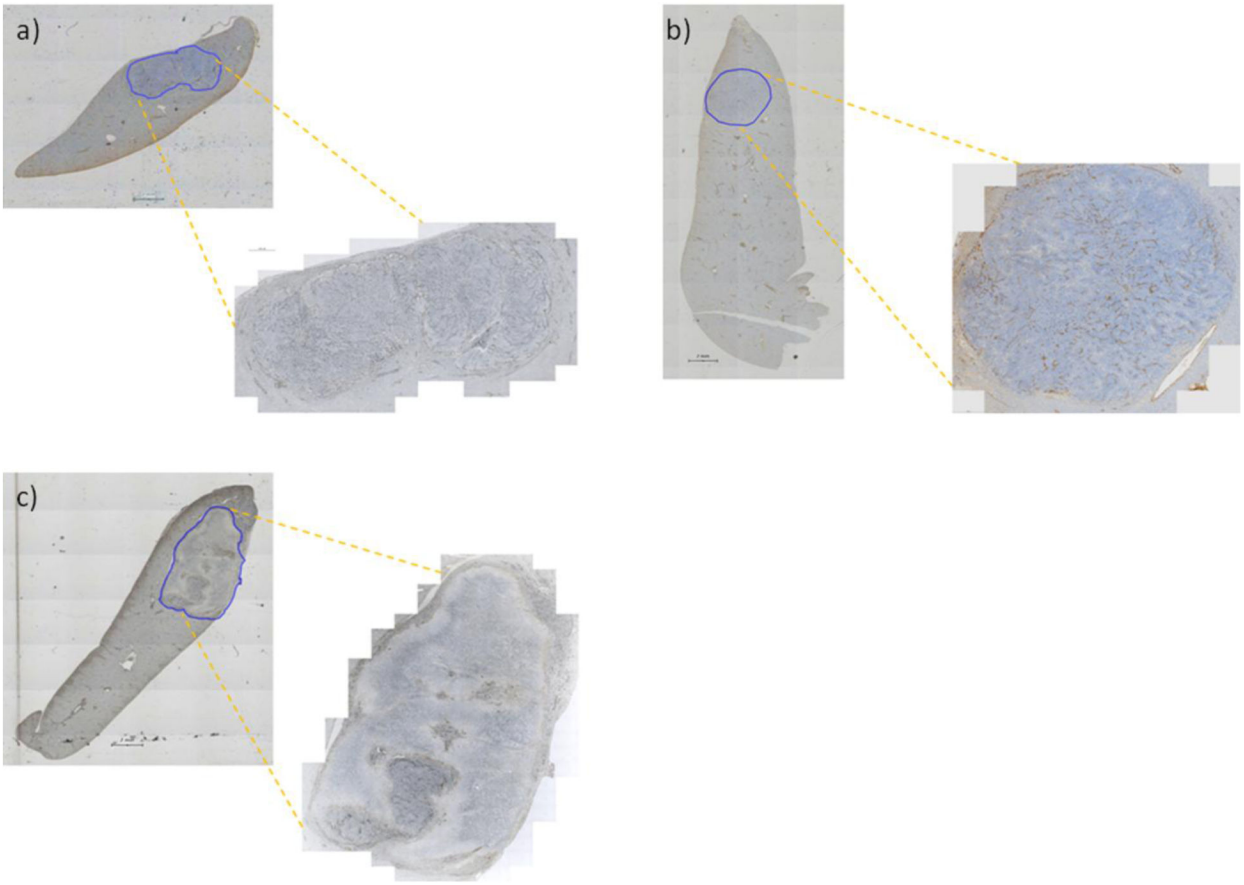

Figure 7.

Immunohistochemistry measurements with anti-CD34 staining demonstrated significantly reduced microvessel density within treatment group tumors compared to both sham and control group tumors. Representative examples from control (**A**), sham (**B**), and treatment (**C**) animals include both a 25x cross-sectional liver slice preview image along with a 200x image of the tumor tissue region from within each corresponding slice.